Tomographic Imaging Spectroscopy of the Solar Transition Region and Corona

Charles C. Kankelborg

HSD Seminar
NASA/GSFC, February 22, 2023

Abstract

Emission lines from soft x-ray to far ultraviolet wavelengths (XUV, $\sim 1 - 200\,\mathrm{nm}$) allow us to observe the solar transition region and corona continuously from space. Images reveal an atmosphere that is magnetically dominated and highly dynamic. The composition, temperature, density, and velocity distribution of the plasma may be inferred from spectra. However, marrying imaging with spectroscopy is inherently challenging, yet more so at XUV wavelengths. XUV imaging spectrsoscopy has mostly been carried out with stigmatic slit spectrographs, which can build up a 2D field of view only gradually, by rastering. I will survey a radical new approach, computed tomography imaging spectroscopy (CTIS), which marries a slitless spectrograph with computational inversion techniques to obtain a spectrum in every pixel of a 2D image. A variety of XUV CTIS instruments have been proposed for solar physics, and several have flown on sounding rockets, yielding observatons of the solar atmosphere in unprecedented spatial-spectral detail. I will conclude with a framework for thinking through the challenges of CTIS, tailoring the instrument configuration and analysis techniques to the science objectives.

Outline

1. XUV observation of the solar TR & Corona
2. Imaging spectroscopy with a slit
3. Imaging spectroscopy without a slit
4. Computed Tomography Imaging Spectrometry (CTIS)
5. Example: MOSES
6. Example: ESIS
7. Example: COSIE
8. Summary

MONTANA STATE UNIVERSITY

Observing in XUV

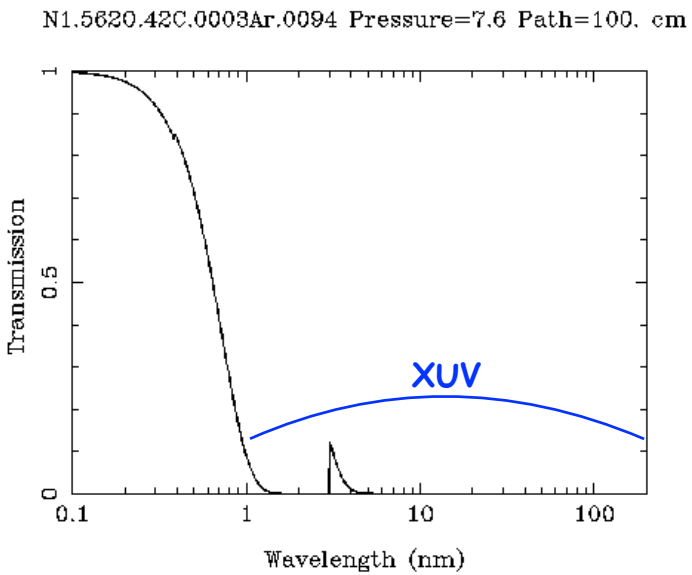

Strongly absorbed in air, even at mechanical vacuum. [1]

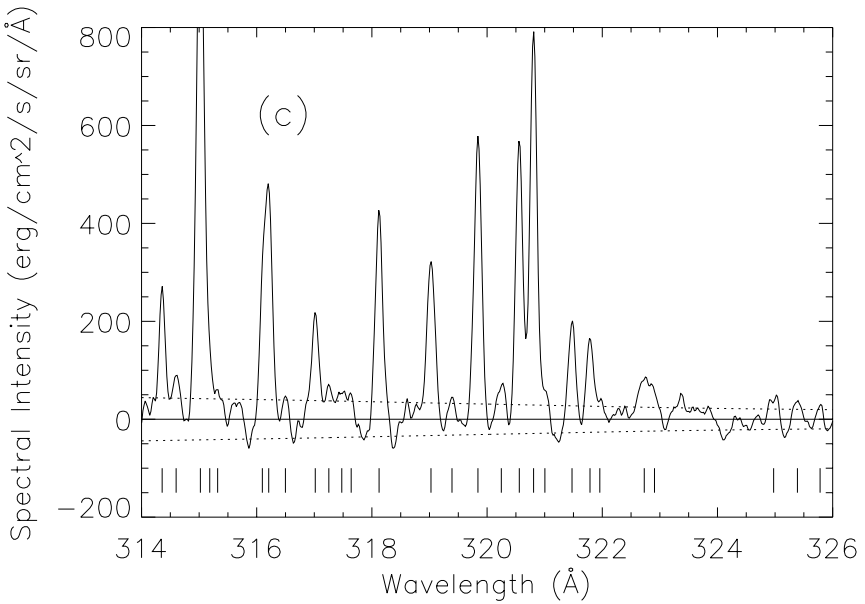

EUV emission line spectrum of an active region (Brosius, Thomas & Davila 2000 [2])

MONTANA STATE UNIVERSITY

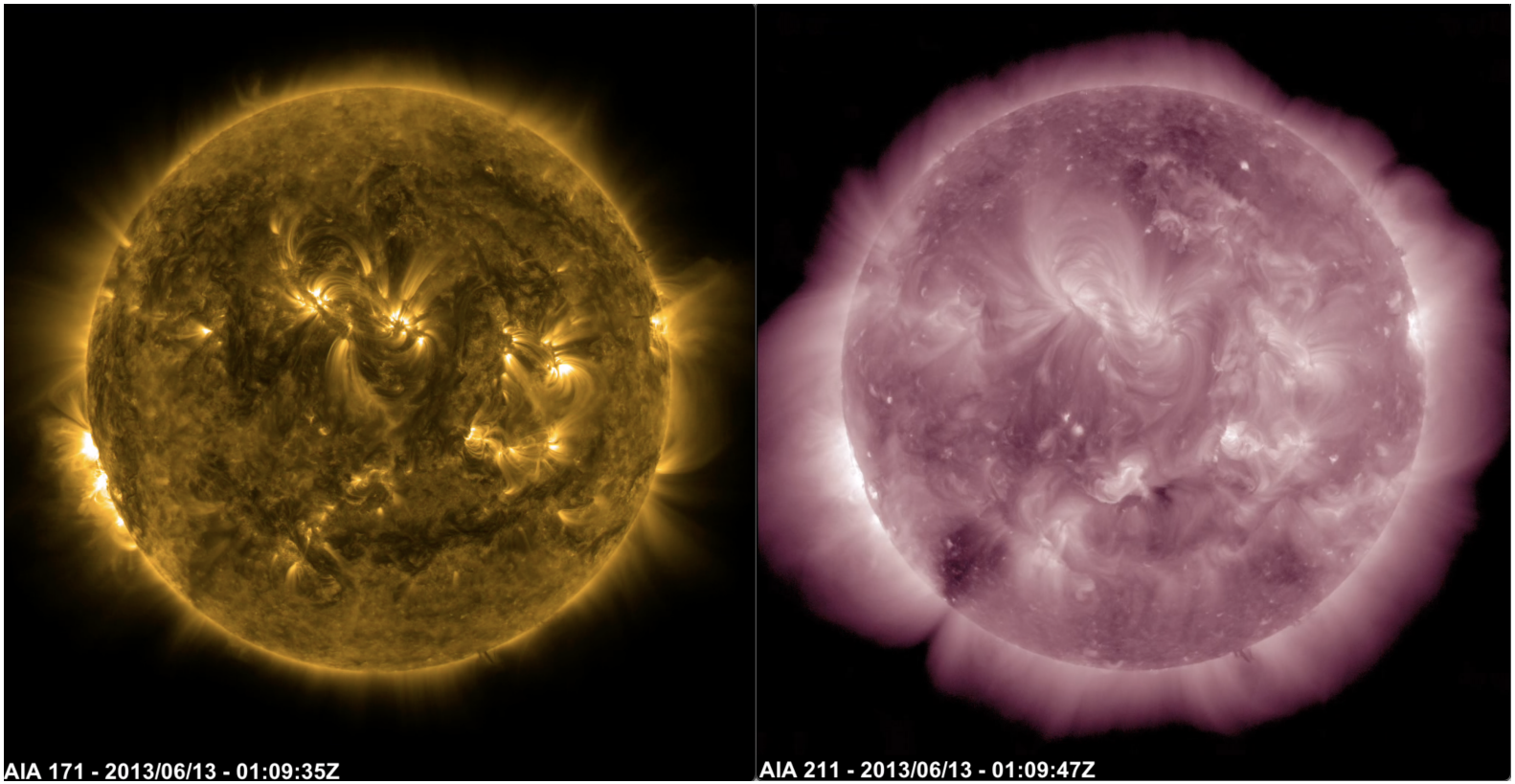

EUV imaging. Multilayer coatings cannot isolate lines, but 171 Å is dominated by Fe IX and 211 Å by Fe XIV. See, e.g., O'Dwyer et al. 2010 [3].

To do physics, we need spectroscopy!

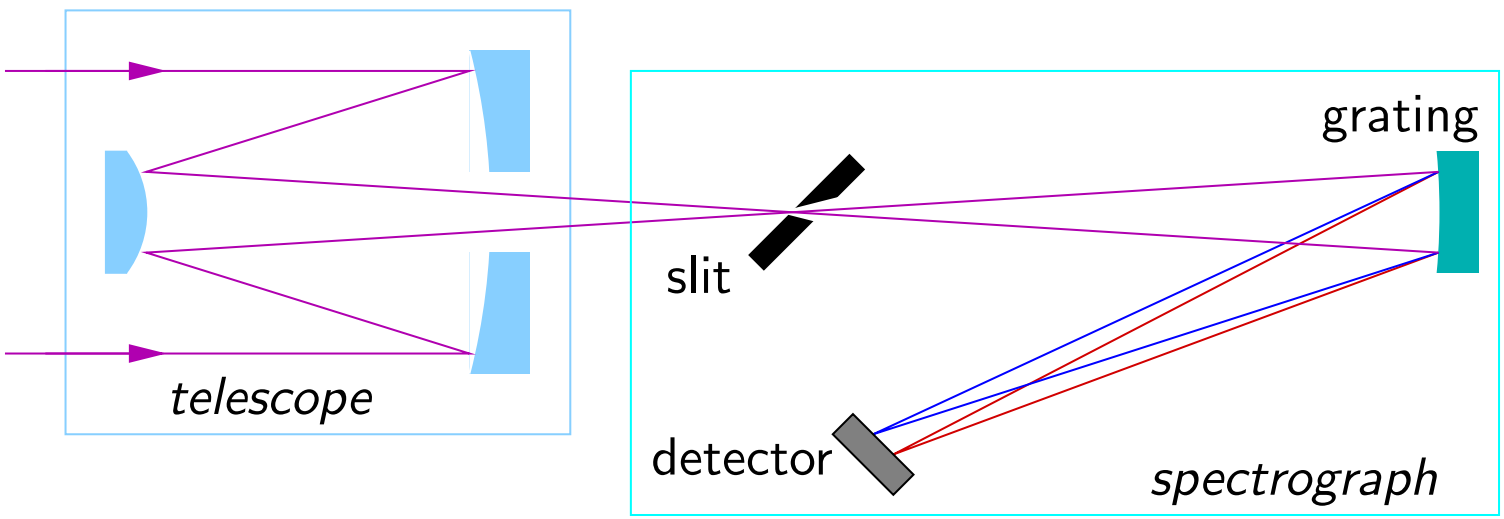

MONTANA STATE UNIVERSITY

Slit Spectrograph

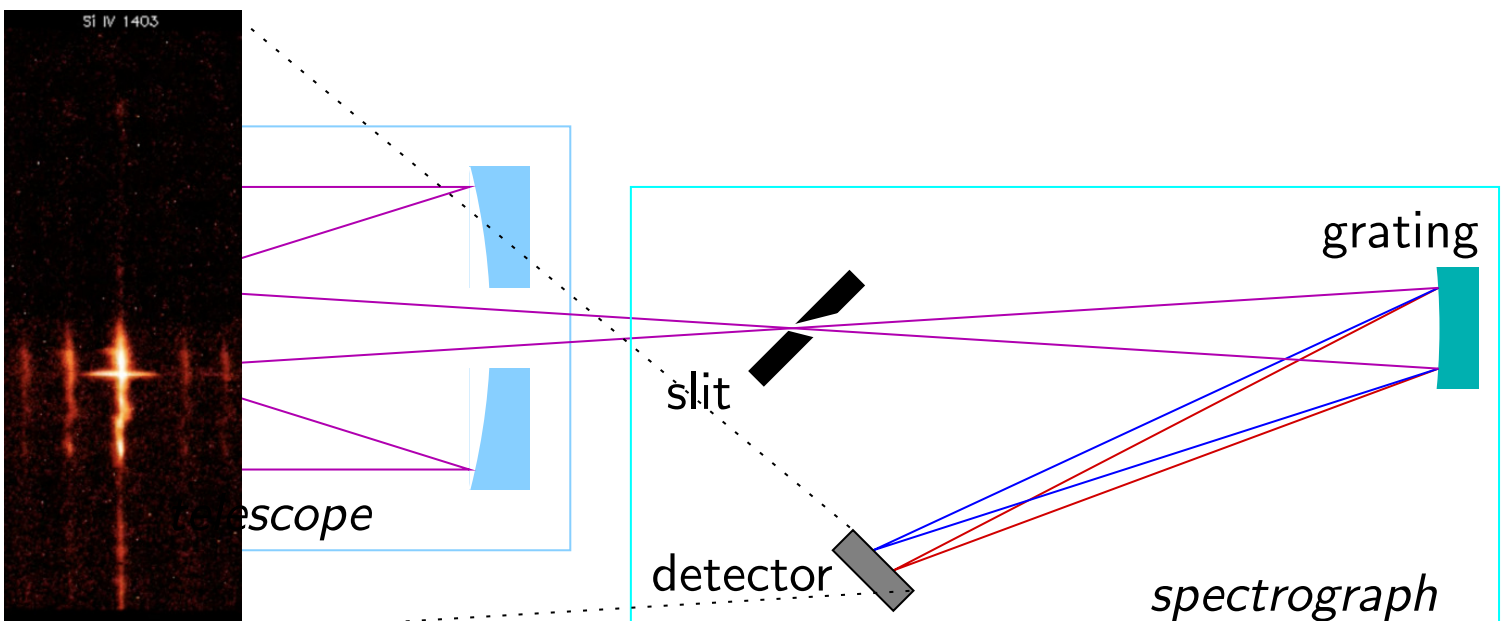

MONTANA STATE UNIVERSITY

Slit Spectrograph

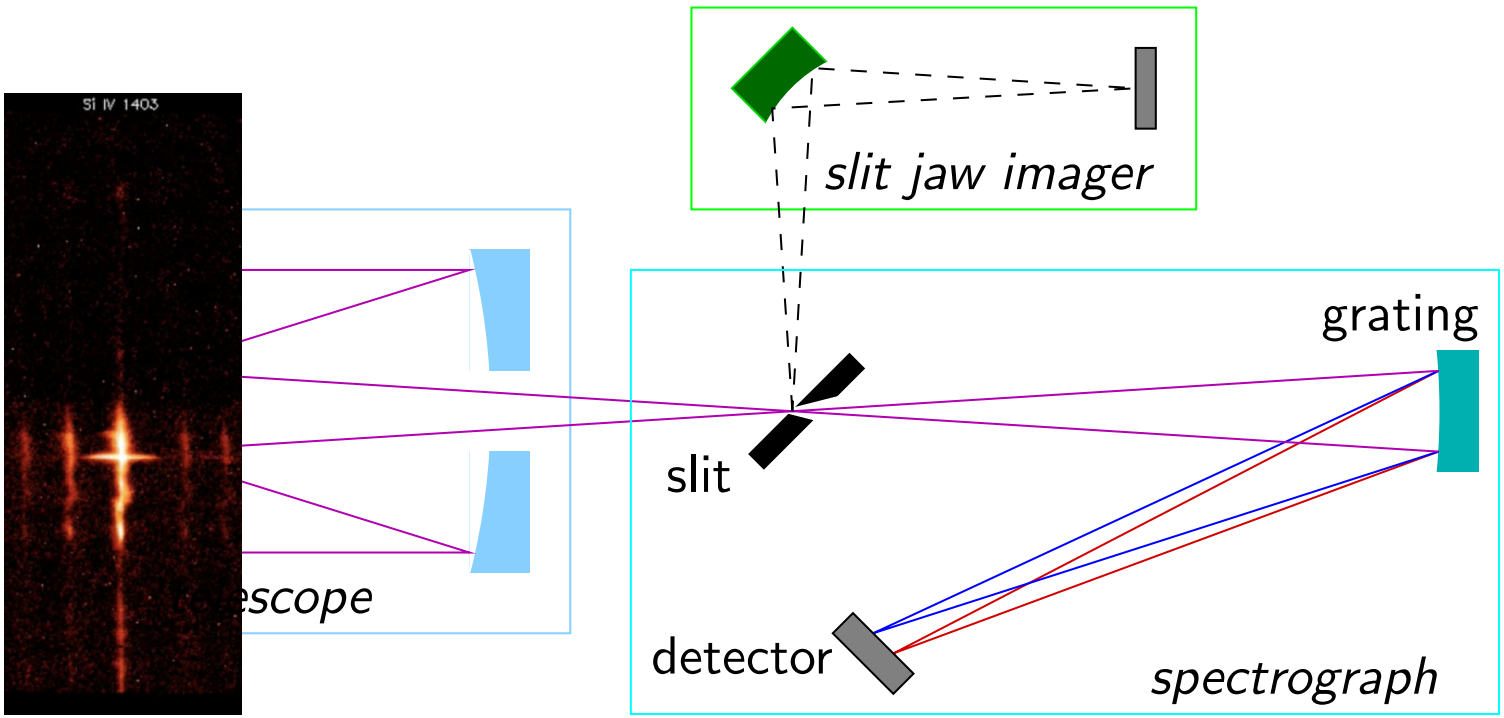

MONTANA STATE UNIVERSITY

Slit Spectrograph

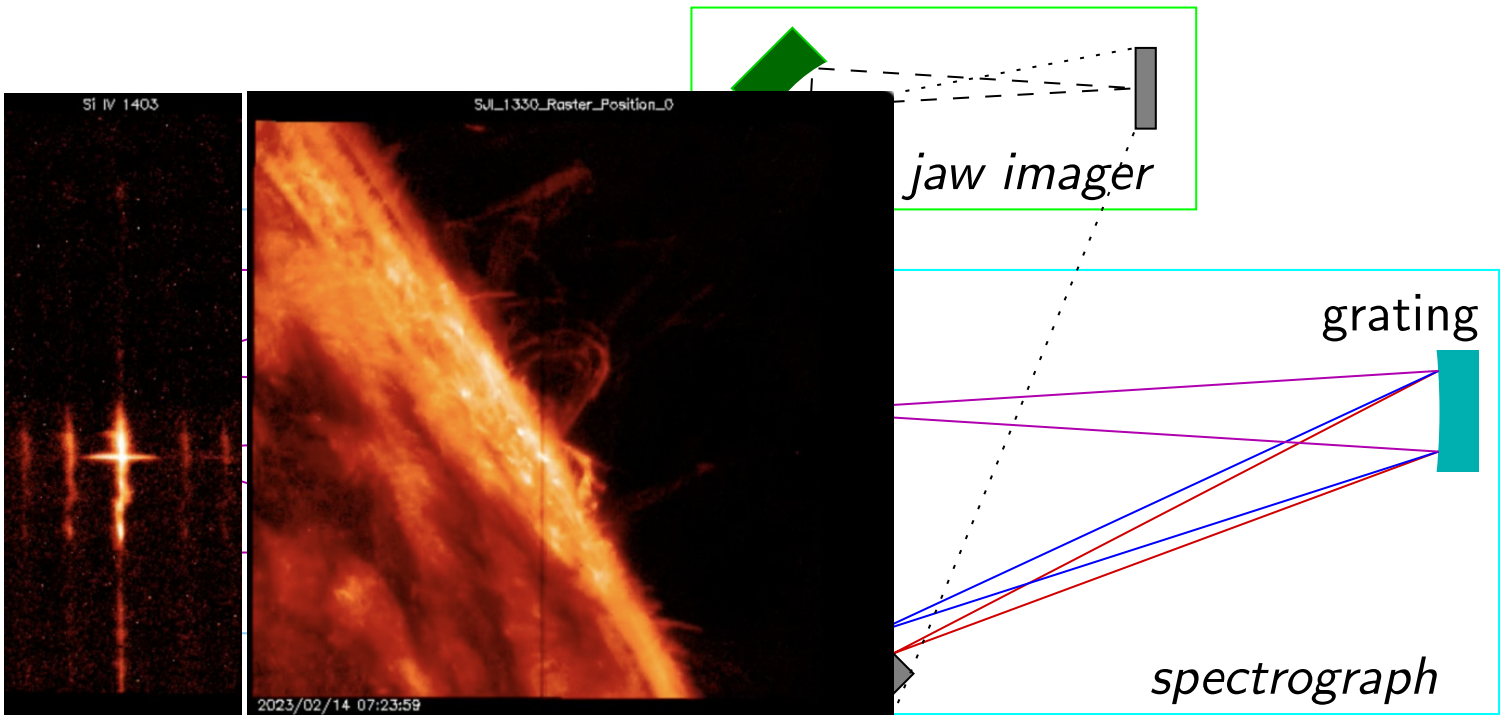

MONTANA STATE UNIVERSITY

Case Study: IRIS

The IRIS slit-jaw imager provides spatial context surrounding stigmatic slit specra.

Brannon, Longcope & Qiu 2015 [4] observed the spatio-temporal undulation of a flare ribbon. The doppler shift of the ribbon (not shown) oscillated in phase with the sky plane motions.

In **sit-and-stare mode**, velocities could be measured at only one point along the ribbon. **Rastering** would have missed the discovery altogether.

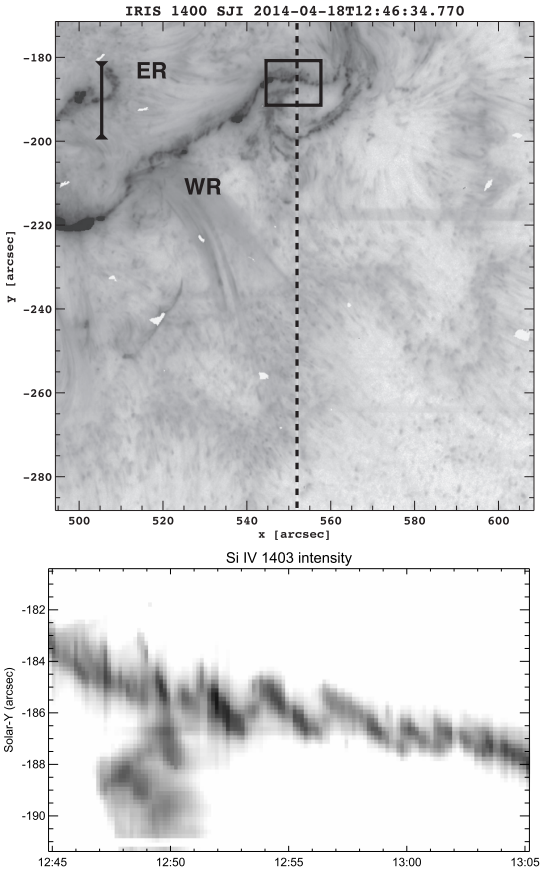

MONTANA STATE UNIVERSITY

Removing the Slit

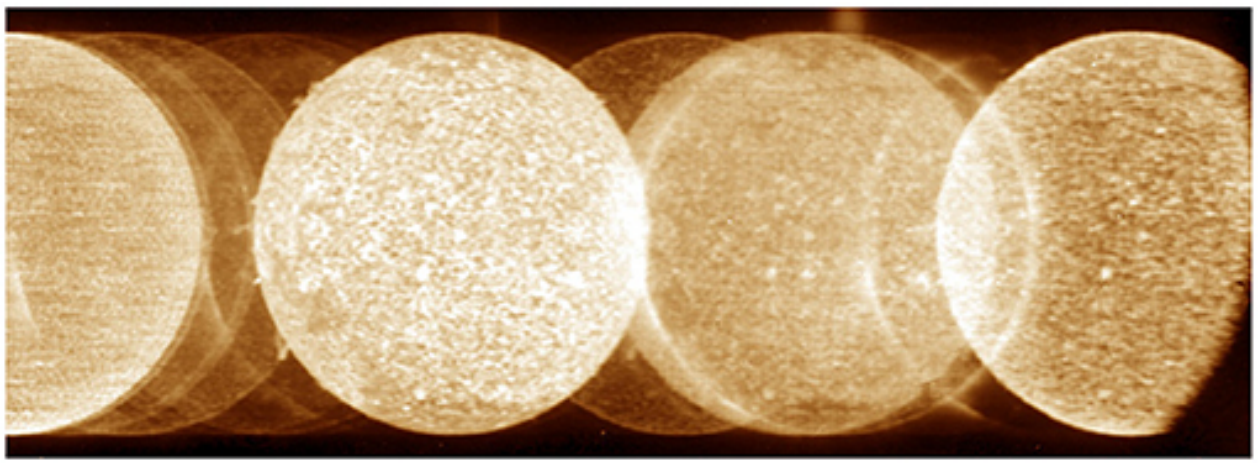

- Skylab S082A (above) [5,6]
- Vis CTIS, Descour & Dereniak 1995 [7]
- Res-K (EUV), Zhitnik et al. 1998 [11]
- Magnetography, DeForest et al. 2004 [10]
- EIS slot, Harra et al. 2017 [8], 2020 [9]

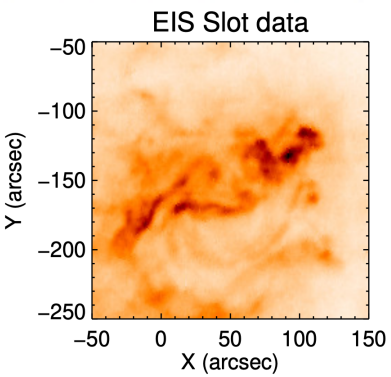

CTIS (Computed Tomography Imaging Spectrometer)

CTIS is a slitless imaging spectrograph that forms multiple 2D projections through (x, y, λ), combined with automated inversion to transform the projections into a higher dimensional data product [7].

The XUV emission spectrum of the solar TR and corona is a promising domain for CTIS:

- The (x, y, λ) cube is sparse in λ (zeroes between emission lines).
- Solar images are highly structured—which facilitates triangulation.

CTIS for the Solar TR and Corona

Solar XUV CTIS Instruments

Instrument	PI/IS	Status	Ref	Comments
MOSES	Kankelborg	Flew '06, '15	[12]	EUV velocities
ESIS	Kankelborg	Flew '19	[19]	EUV velocities
MaGIXS	Winebarger	Flew '21	[16]	Soft X-ray
MOXSI	Caspi	Funded	[17]	Soft X-ray
COSIE	Golub	Under study	[20]	EUV (V)DEM
COOL-AID	Golub/Samra	Funded	[6]	EUV (V)DEM

MOSES: Multi-Order Solar EUV Spectrograph (304 Å)

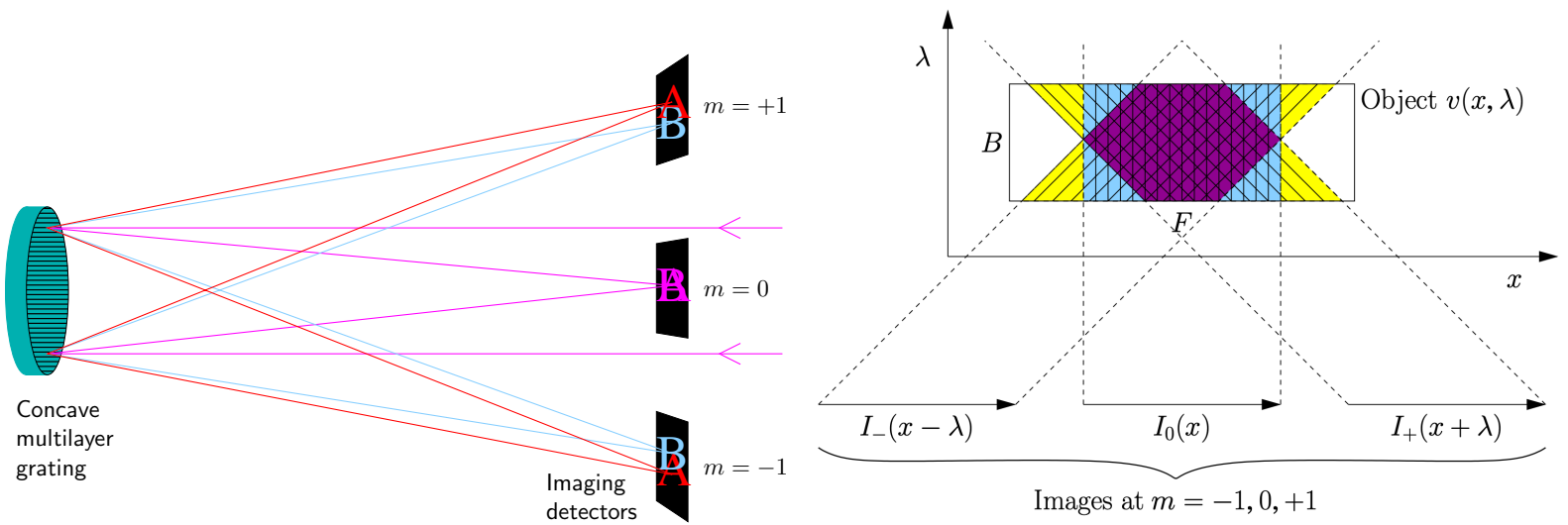

The concept behind the MOSES sounding rocket instrument.
Fox, Kankelborg & Thomas 2010 [12]

MONTANA STATE UNIVERSITY

MOSES: Image Differences & Fitting

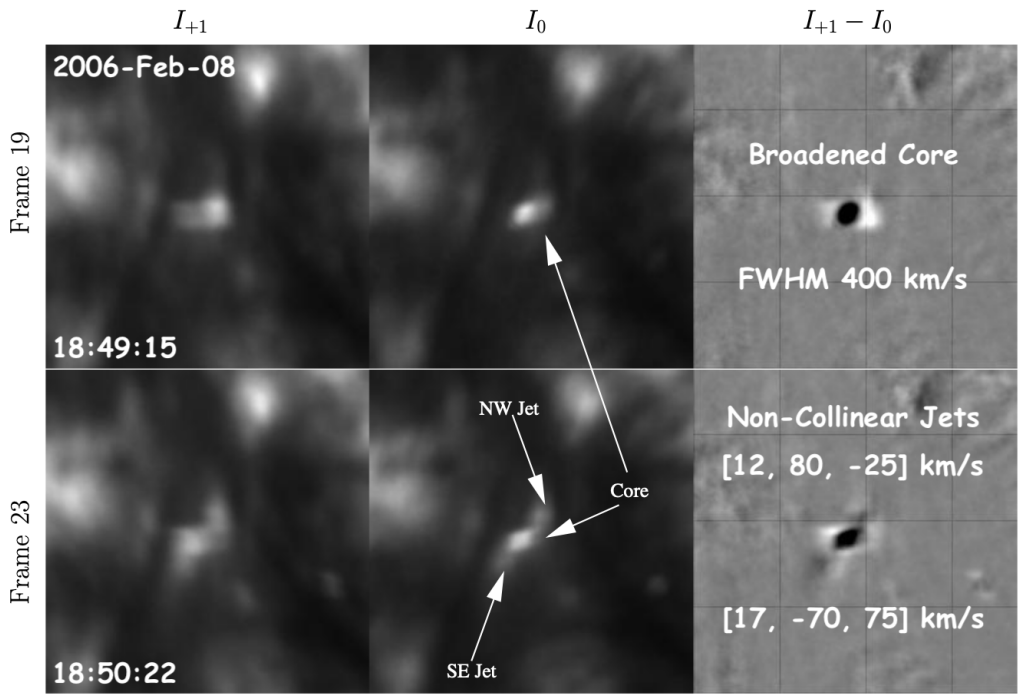

He II explosive event. Fox, Kankelborg & Thomas 2010 [12].

MONTANA STATE UNIVERSITY

MART: Multiplicative Algebraic Reconstruction Technique

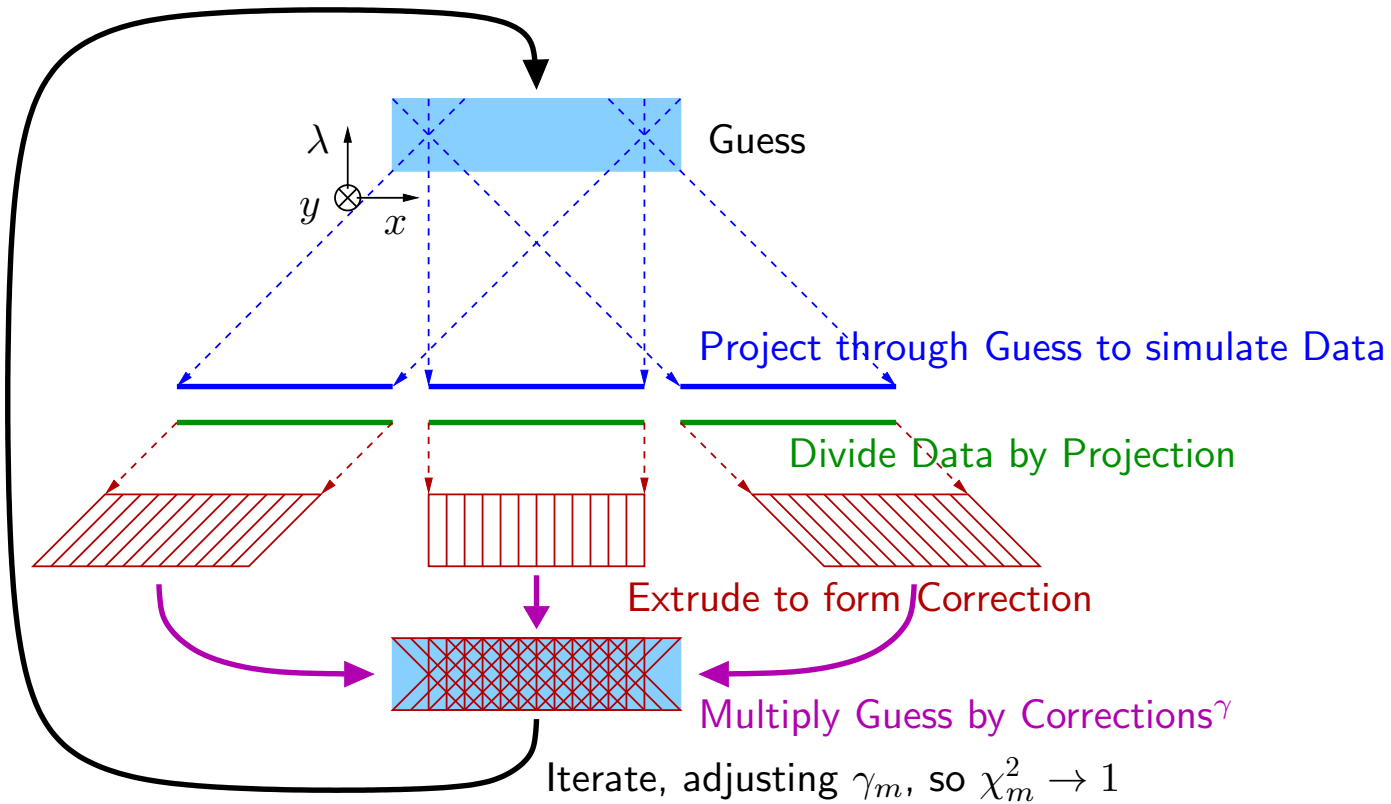

MONTANA STATE UNIVERSITY

MOSES: What have we learned so far?

- Science
  - Two-phase explosive event [12]
  - Tens of bimodal explosive events - Rust & Kankelborg (2019) [14]
  - MOSES-II, Ne VII downflow
- Undispersed ($m = 0$) channel improves spatial resolution.
- Passband defined by multilayers, but...
- Off-band lines from beyond FOV - Parker & Kankelborg 2022 [18]

Analysis methods:

- Image differences - Fox et al. (2010) [12]
- Hand-fitting blobs [12]
- Pixons - Fox, Kankelborg & Metcalf (2003) [13]
- MART - Fox, Rust
- Doppler shift via correlation tracking - Courrier [15]
- Convolutional Neural Networks (in progress) - Smart

ESIS: EUV Snapshot Imaging Spectrograph (630 Å)

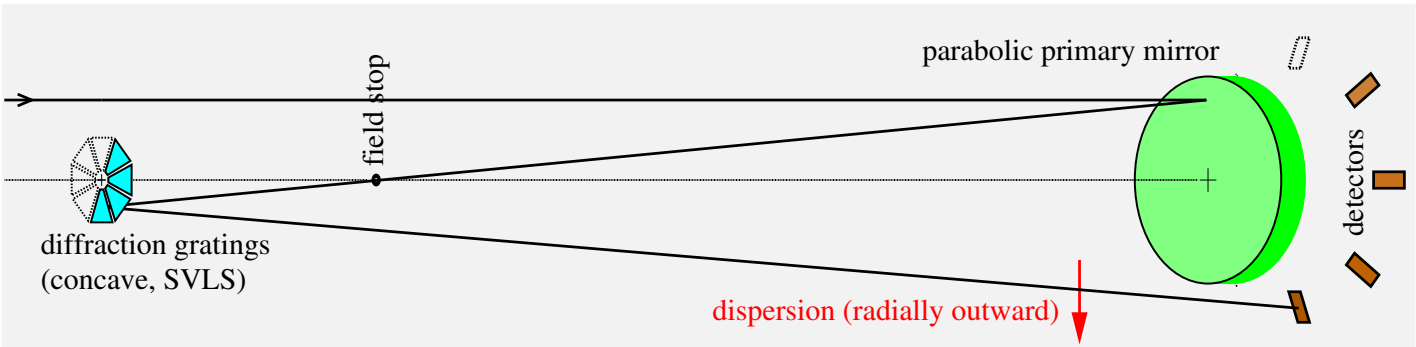

- Pseudo-Gregorian layout, with field stop.
- Rely on grating dispersion + field stop to limit passband.
- One grating per channel. VLS gratings minimize aberration.

- No undispersed image.
- 4 dispersion planes at 45° intervals maximize spatial resolution and minimize spectral confusion.
- MART inversion with iterative contrast enhancement suppresses "plaid" artifacts.

MONTANA STATE UNIVERSITY

ESIS: EUV Snapshot Imaging Spectrograph (630 Å)

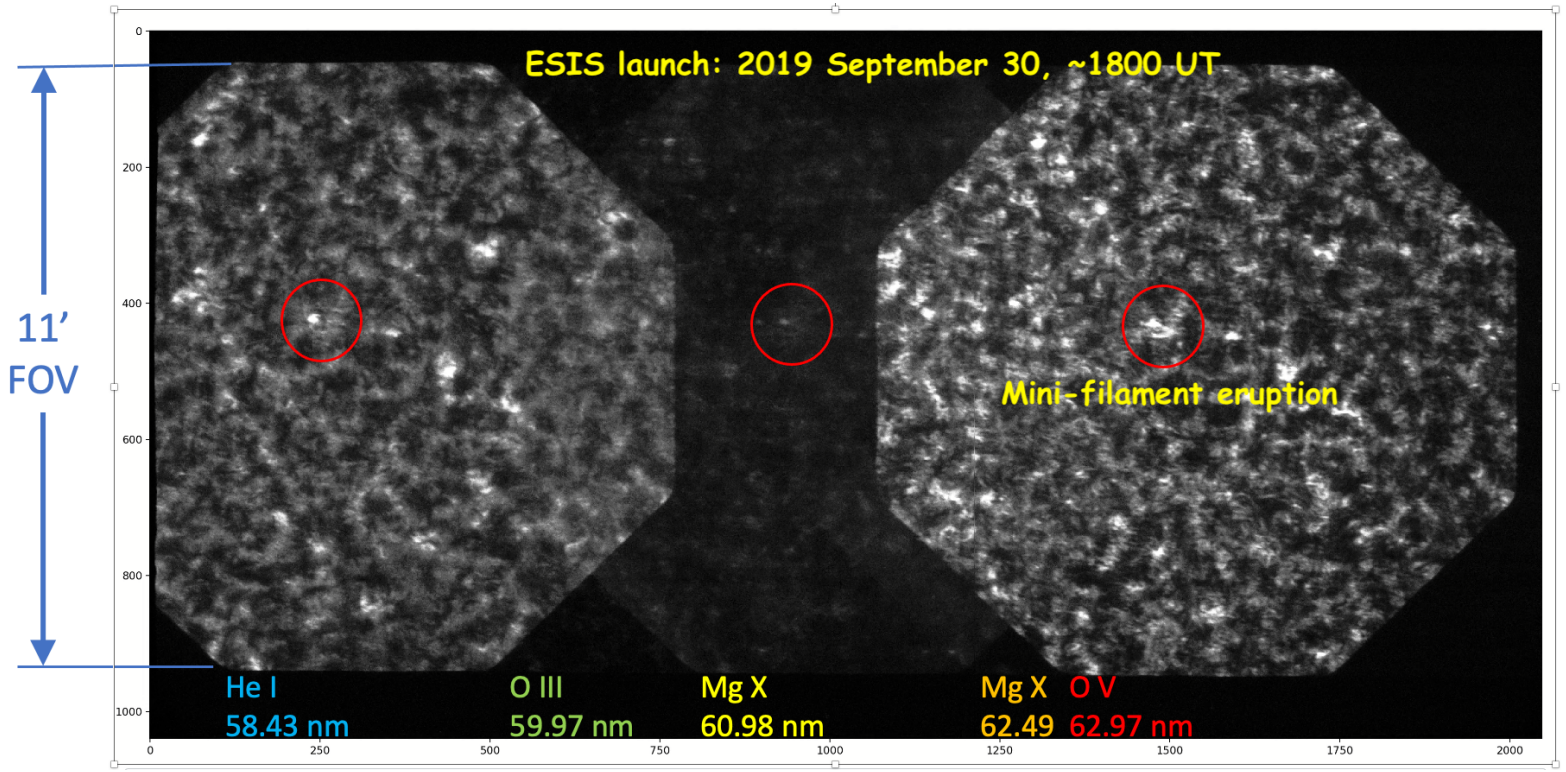

MONTANA STATE UNIVERSITY

ESIS: Explosive Event in O V

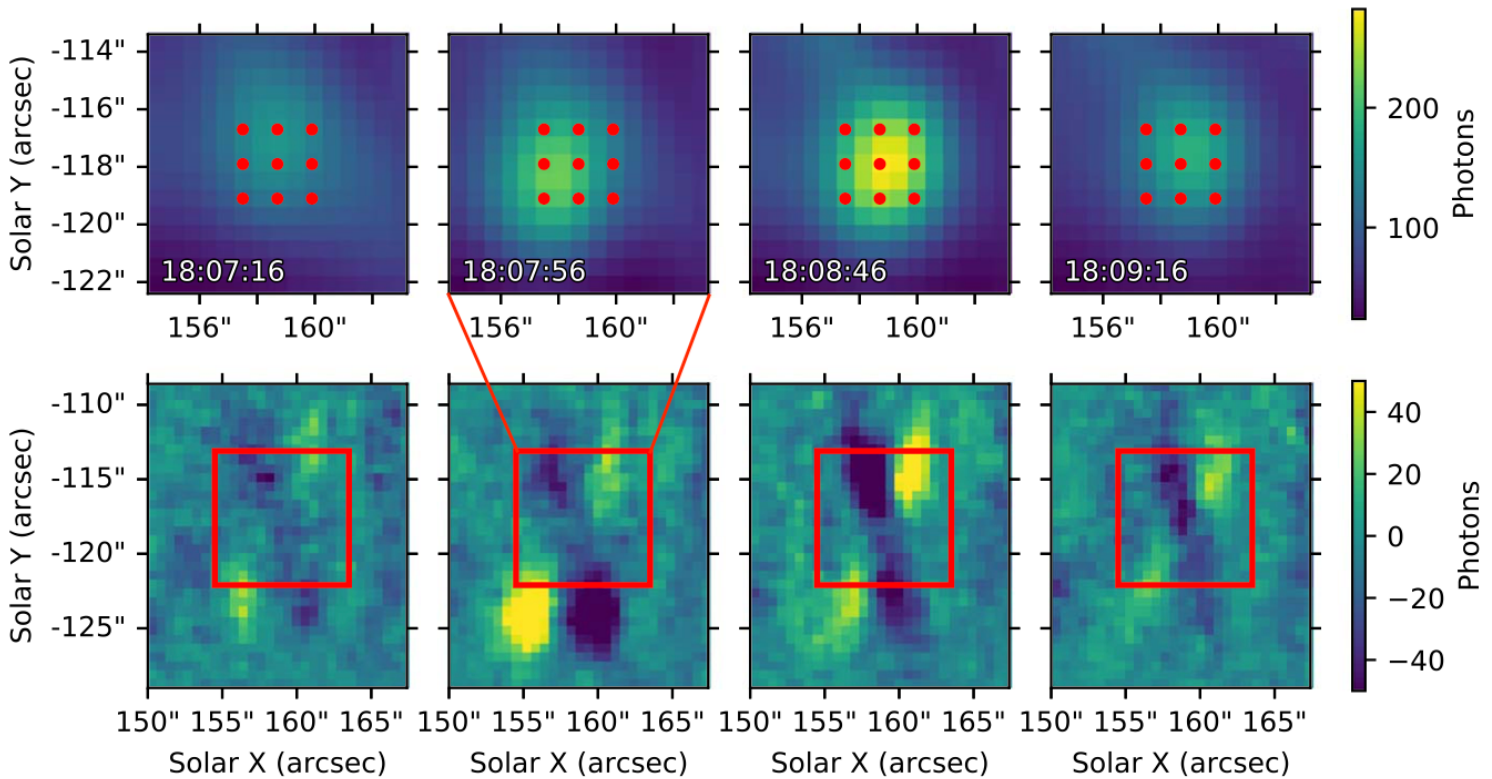

MONTANA STATE UNIVERSITY

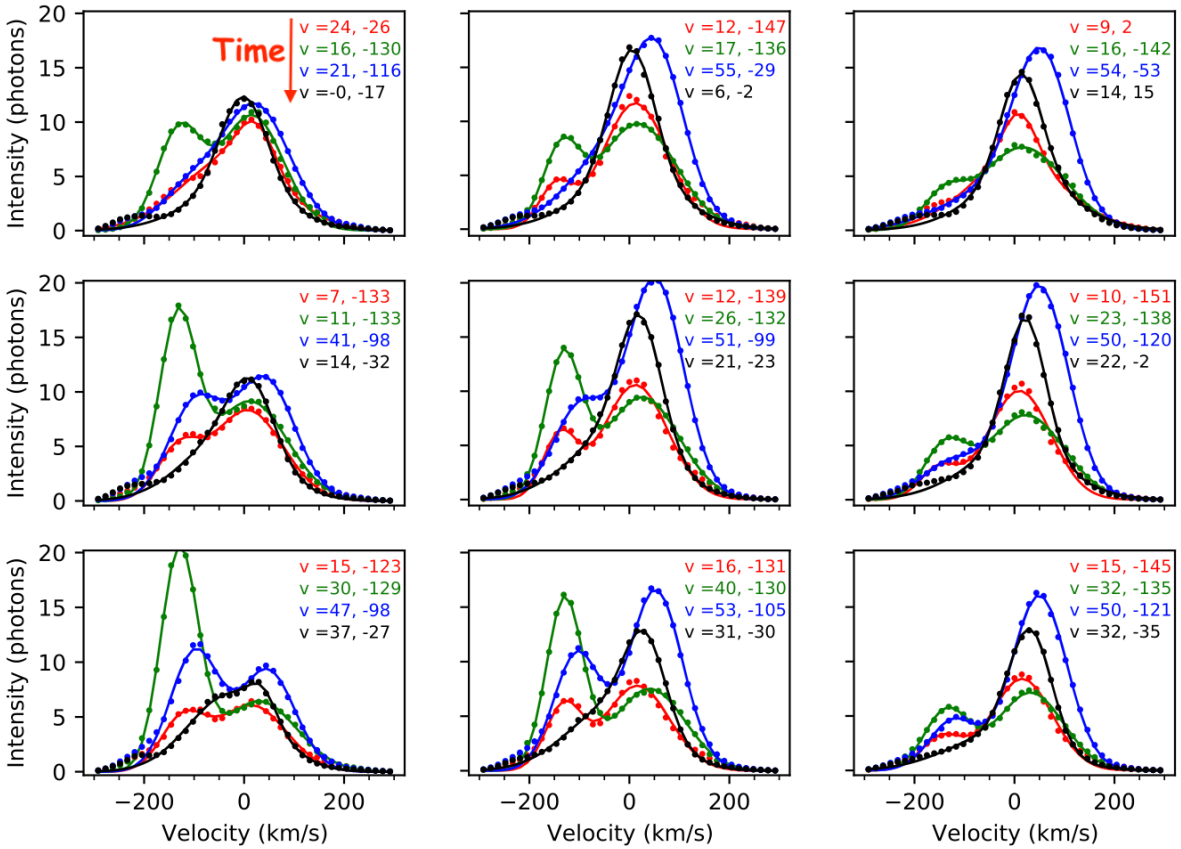

MART inversion of bimodal event, with a blue-shifted jet in the SE (green) and a weaker, central red-shifted jet peaking $\sim 50\,\mathrm{s}$ later (blue).

MONTANA STATE UNIVERSITY

COSIE: COronal Spectroscopic Imager in the EUV

- Many lines, prioritizing intensity over velocity resolution.
- EW direction has $3\times$ resolution of NS (dispersion) direction.
- One dispersed channel (right), one undispersed.
- Inversion: LASSOLARS solves for DEM at every (x, y). This enforces consistency in the recovered line intensities.
- Regularization: Minimize total EM (I suspect this suppresses "plaid").
- Constrains density & perhaps velocity (VDEM).
- COOL-AID (COSIE$\times 2$) on Hi-C Flare, 2024!

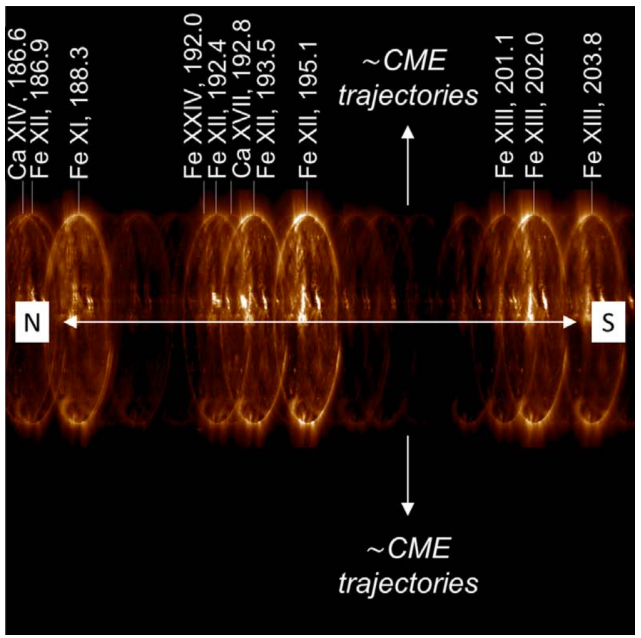

COSIE is a proposed MOO to study CME acceleration – Winebarger 2019. [20]

MONTANA STATE UNIVERSITY

Summary: CTIS for the TR and Corona

A growing body of work demonstrates XUV imaging and spectroscopy across a wide field in a single exposure. There are many trade-offs, in instrument design and in data analysis.

Instrument configuration options:

- Few lines, high dispersion (profiles).
- Many lines, low dispersion (ratios).
- More projections $\Longrightarrow$ more information.
- Vary dispersion angle (spatial resolution; spectral disambiguation).
- Undispersed image ('zero order').
- Field stop.

Promising inversion strategies:

- Quicklook: image differences.
- Fast doppler maps via LCT.
- MART $\rightarrow I(x, y, \lambda)$; "Plaid" artifacts, endemic to few-angle tomography, can be suppressed.
- CNN show promise for complex line profiles (so far on training data).
- LASSOLARS $\rightarrow$ (V)DEM.

MONTANA STATE UNIVERSITY

References

1. https://henke.lbl.gov/optical_constants/
2. Brosius, J. W., Thomas, R. J., Davila, J. M. (2000) ApJ 543:1016ff.
3. O'Dwyer, B., Del Zanna, G., Mason, H. E., Weber, M. A., Tripathi, D. (2010) A&A 521, A21
4. Brannon, S. R., Longcope, D. W., Qiu, J. (2015) ApJ 810:4.
5. Tousey, R., Bartoe, J.-D. F., Brueckner, G. E., Purcell, J. D., 1977 ApOpt, 16:870T
6. Young, P. (2021) Front. Astron. Space Sci., 8
7. Descour, M. R., Dereniak, E. L. (1995) Proc. SPIE, 2480, 48
8. Harra, L., Hara, H., Doschek, G. A., Matthews, S., Warren, H., Culhane, J. L., Woods, M. M. (2017) Apj 842,1,58
9. Harra, L., Matthews, S., Long, D., Hasegawa, T., Lee, K.-S., Reeves, K., Shimizu, T., Hara, H., Woods, M. (2020) Sol. Phys. 295:34

10. Deforest, C. E., Elmore, D. F., Bradford, M. P., Elrod, J., Gilliam, D. L. (2005) ApJ 616:600
11. Zhitnik, I. A., Kuzin, S. V., Oraevskii, V. N., et al. (1998) Astron. Let. 24, 819

12. Fox, J. L., Kankelborg, C. C., Thomas, R. J. (2010) ApJ 719:832
13. Fox, J. L., Kankelborg, C. C., Metcalf, T. R. (2003) Proc. SPIE 5157:124ff
14. Rust, T., Kankelborg, C. C. (2019) ApJ 877:59
15. Courrier, H. T., Kankelborg, C. C. (2018) JATIS 4:018001
16. Savage, S. L., Winebarger, A. R., Kobayashi, K., Athiray, P. S. et al. (2022) arXiV 2212:00665
17. Caspi, A., Shih, A. Y., Warren, H. P., Steslicki, M., Sylwester, J. (2017) `https://arxiv.org/abs/1701.00619`
18. Parker, J. D., Kankelborg, C. C. (2022) ApJ 932:130
19. Parker, J. D., Smart, R. T., Kankelborg, C. C., Winebarger, A., Goldsworth, N. (2022) ApJ 938:116

20. Winebager, A. R., Weber, M., Bethge, C., Downs, C., Golub, L., DeLuca, E., Savage, S., delZanna, G., Samra, J., Madsen, C., Ashraf, A., Carter, C. (2019) ApJ 882:12

Backup Slides

MOSES: Anomalous Spectral Content

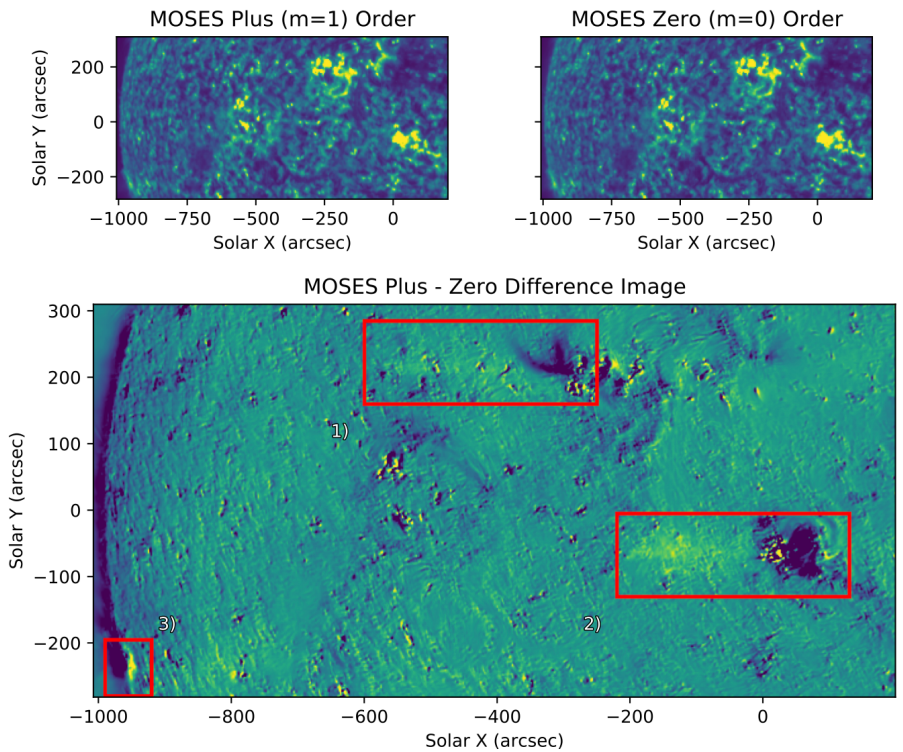

MOSES: Anomalous Spectral Content

Table 1
Pixel Dispersion of Dominant Spectral Lines with Intensities Relative to He II 303.78 Å

Spectral Line	Relative Intensity (%)	Dispersion (pixels)	Dispersion (arcsec)
Si IX 292.80 Å	0.19	−378.62	−227.17
Si IX 296.12 Å	1.42	−264.24	−158.54
Si IX 296.21 Å	0.46	−260.93	−156.56
Si XI 303.32 Å	15.59	−15.69	−9.41
Fe XIII 303.36 Å	0.62	−14.34	−8.61
He II 303.78 Å	100.00	0.00	0.00
He II 303.79 Å	49.91	0.21	0.12
Al IX 305.05 Å	0.18	43.62	26.17
Si VIII 308.19 Å	0.29	152.03	91.22
Fe XI 308.54 Å	1.04	164.28	98.57
Fe XIII 311.55 Å	0.19	267.83	160.70
Mg VIII 311.77 Å	1.26	275.59	165.35
Fe XIII 312.17 Å	0.94	289.45	173.67
Fe XIII 312.87 Å	0.36	313.38	188.03
Mg VIII 313.74 Å	1.91	343.55	206.13
Si VIII 314.36 Å	1.69	364.69	218.81
Mg VIII 315.01 Å	3.99	387.41	232.45
Si VIII 316.22 Å	2.16	428.90	257.34
Mg VIII 317.03 Å	0.53	456.83	274.10
Si VIII 319.84 Å	0.66	553.76	332.26

Table 2
Average MOSES Image Spectral Content

Ion	Contribution
He II	80.55%
Si XI	8.37%
Mg VIII	4.14%
Si VIII	2.65%
Si IX	1.33%
Fe XIII	1.29%
Other	1.67%

5. Discussion and Conclusions

MOSES was successful in its goal of capturing solar images in the He II 303.8 Å emission line. Despite the use of a narrowband multilayer coating on both the primary and secondary optics, MOSES captured several solar features not easily attributed to the dominant He II 303.8 Å or nearby strong Si XI 303.3 Å lines. In order to identify and quantify the spectral content of these additional features, we cross-correlated two MOSES difference images and identified peaks in correlation as significant and indicative of spectral contamination. Using a forward model that combines four cotemporal EIT images with synthetic spectra from Chianti, we created synthetic MOSES difference images with known spectral content that could be cross-correlated and compared to the MOSES difference image cross-correlation function. By

MONTANA STATE UNIVERSITY